JOURNAL OF ENDOUROLOGY
Volume 37, Number 10, October 2023

Pp. ■■■–■■■
DOI: 10.1089/end.2023.0215

Original Research

Open camera or QR reader and scan code to access this article and other resources online.

Periprostatic Adipose Tissue MRI Radiomics-Derived Features Associated with Clinically Significant Prostate Cancer

Mohammed Shahait, MBBS,[1] Ruben Usamentiaga, PhD,[2] Yubing Tong, PhD, Senior IEEE Member,[3]
Alex Sandberg, BS,[4] David I. Lee, MD,[5]
Jayaram K. Udupa, PhD, LFIEEE, FAIMBE,[3] and Drew A. Torigian, MD, MA, FSAR[3]

Abstract

Background: Altered systemic and cellular lipid metabolism plays a pivotal role in the pathogenesis of prostate cancer (PCa). In this study, we aimed to characterize T1-magnetic resonance imaging (MRI)-derived radiomic parameters of periprostatic adipose tissue (PPAT) associated with clinically significant PCa (Gleason score ≥7 [3+4]) in a cohort of men who underwent robot-assisted prostatectomy.
Methods: Preoperative MRI scans of 98 patients were identified. The volume of interest was defined by identifying an annular shell-like region on each MRI slice to include all surgically resectable visceral adipose tissue. An optimal biomarker method was used to identify features from 7631 intensity- and texture-based properties that maximized the classification of patients into clinically significant PCa and indolent tumors at the final pathology analysis.
Results: Six highest ranked optimal features were derived, which demonstrated a sensitivity, specificity, and accuracy of association with the presence of clinically significant PCa, and area under a receiver operating characteristic curve of 0.95, 0.39 0.82, and 0.82, respectively.
Conclusion: A highly independent set of PPAT features derived from MRI scans that predict patients with clinically significant PCa was developed and tested. With future external validation, these features may provide a more precise scientific basis for deciding to omit biopsies in patients with borderline prostate-specific antigen kinetics and multiparametric MRI readings and help in the decision of enrolling patients into active surveillance.

Keywords: radiomics, MRI, prostate cancer

Introduction

Prostate cancer (PCa) is the most commonly diagnosed malignancy in men and is considered the fifth leading cause of cancer-related mortality in Western countries.[1] One of the major challenges in the management of patients with suspected PCa is confirming the diagnosis by performing a biopsy. A substantial number of patients with suspected PCa may undergo unnecessary biopsies, where clinically insignificant cancers are often detected and clinically significant cancers are sometimes missed.[2] Over the years, several efforts have been made to optimize PCa biopsy by using extended templates, tumor markers, incorporating multiparametric magnetic resonance imaging (mpMRI), and targeted biopsies in the prostate biopsy pathway.[3]

mpMRI of the prostate provides anatomical information about the lesion location within the prostate and its relation to the neurovascular bundle and urethra. In addition, it provides

[1]Department of Surgery, Clemenceau Medical Center, Dubai, United Arab Emirates.
[2]Department of Computer Science and Engineering, University of Oviedo, Gijon, Spain.
[3]Medical Image Processing Group, Department of Radiology, University of Pennsylvania, Philadelphia, Pennsylvania, USA.
[4]Temple Medical School, Temple University, Philadelphia, Pennsylvania, USA.
[5]Department of Urology, University of California Irvine, Irvine, California, USA.

data on tumor characteristics, such as enhancement, vascularity, and metabolite.[4] There is growing evidence showing that mpMRI tends to detect high-grade disease and systematically overlooks low-grade disease. However, mpMRI still fails to detect a significant proportion of high-grade tumors.[5]

Altered systematic and cellular lipid metabolism plays a pivotal role in the pathogenesis of PCa. Recent evidence has shown that periprostatic adipose tissue (PPAT) affects the prostate microenvironment by either a paracrine effect or cell-to-cell interactions.[6] Several studies have shown an association between the total PPAT area and density with high-risk PCa at the final pathology analysis.[7–10] Conversely, other studies found no correlation between PPAT density and aggressive PCa.[6]

We theorized that preoperative MRI-derived radiomic features of PPAT, obtained using an optimal biomarker (OBM) approach, might help identify patients with clinically significant PCa. In this study, we sought to characterize the MRI-derived radiomic features of PPAT associated with clinically significant PCa (Gleason score, GS ≥7 [3 + 4]) in a cohort of men who underwent robot-assisted prostatectomy.

Methods

Study population

This retrospective study was approved by the institutional review board of our institution. We identified 140 patients who underwent robot-assisted prostatectomy at a single institution between 2013 and 2018. All patients underwent preoperative mpMRI, did not receive any neoadjuvant treatment, or had undergone prior surgery. Patients were excluded ($N = 42$) if they had suboptimal imaging quality or missing T1 sequences. Only nonfat-suppressed small field-of-view T1-weighted axial MR images were used in this study.

The MRI scans were acquired for clinical purposes on 1.5 to 3.0 Tesla Siemens clinical MRI scanners with Espree model and *tse2d1_3 sequence. The axial slice images varied from 192×192 to 512×512 in size, with 18 to 40 slices acquired from the aortic bifurcation to the equator of the femoral heads. The voxel size varied from $0.62 \times 0.62 \times 4\,mm^3$ to $1.48 \times 1.48 \times 12\,mm^3$. The repetition time ranged from 1000 to 6680 ms, and the echo time ranged from 80 to 93 ms. Supplementary Table S1 summarizes patients' characteristics.

Trimming, image intensity standardization, PPAT delineation

The workflow of the proposed method is illustrated in Figure 1. Prostate MRI scans were acquired from the patients. The set of slices in the scan from each patient was then trimmed in a standard manner by excluding slices that did not cover the region of interest. The trimmed data set is then standardized so that the same tissue regions have similar image intensity meanings.[11] Subsequently, in each slice of the trimmed and standardized data set, the PPAT region was manually identified and delineated using the CAVASS software system (Computer-Aided Visualization and Analysis Software System) by a fellowship trained urologist.[12]

Several methods have been employed to delineate PPAT. Most of these studies rely on characterizing the PPAT in one slice to measure different features, such as thickness and density.[6–9] However, the use of one slice image to characterize PPAT assumes that PPAT is homogeneous in tissue properties across slices. After an extensive review of the literature and several videos provided by the senior surgeon (D.I.L.), the authors decided to define PPAT in this study as all surgically resectable visceral adipose tissue anterior to the endopelvic fascia extending from the prostatic base to the apex, while excluding mesorectal and ischiorectal/ischioanal fossa fat.[13]

Software. CAVASS is an advanced and innovative medical image processing software developed by the Medical Image Processing Group (MIPG) at the University of Pennsylvania. Building upon the legacy of their previous system, CAVASS represents the next generation of medical image analysis and observation tools. A core focus of CAVASS lies in its specialization for the observation, processing, and analysis of three-dimensional (3D) and higher dimensional medical imagery. With a strong emphasis on supporting DICOM data and implementing algorithms with optimal efficiency, CAVASS is tailored to the specific needs of medical professionals and researchers.[12]

OBM selection—OBM model

The OBM approach utilized in this study first creates a model in the training stage by using data sets wherein the classification of each patient case as clinically significant or

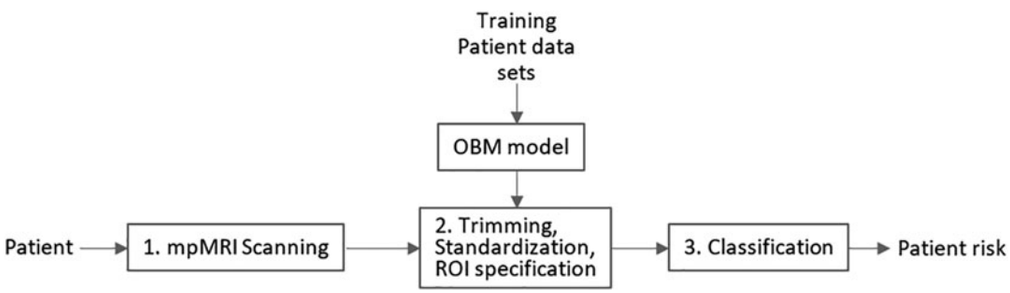

FIG. 1. The proposed radiomic method workflow. Scan data set was trimmed, and in each slice of the trimmed data set, the ROI corresponding to PPAT was manually delineated. To ensure the intensity values in the images have numerical meaning, all images were first corrected for intensity nonuniformities. Then images were standardized in accordance with a standard intensity scale. The parameters of the scale were estimated from control MRI data sets. PPAT = periprostatic adipose tissue; ROI = region of interest.

nonsignificant cancer is known. Subsequently, for any other given test patient data set, the model is utilized to classify the patient into one of two classes.[14]

Three different groups of features computed from the delineated PPAT region were employed in the adaptation of the OBM approach for each patient study: volumetric, image intensity-based, and textural. Intensity-based features are derived from the histogram of image intensities within the PPAT region and include the mean, median, standard deviation, mode, maximum, minimum, quartiles, moments, skewness, kurtosis, and peak height. The textural features derived from the PPAT region textural characteristics were defined using two different types of texture descriptors: local binary pattern (LBP) and gray level co-occurrence matrix (GLCM).[15,16] The total number of features derived in this manner for each patient case was 7631.

To create the OBM model, the OBM approach first selects a small subset of 5 to 10 best performing features from a large set of (7631) features by simultaneously requiring that the selected features satisfy two conditions: (1) they are as least uncorrelated among all features as possible and (2) they hold the best power to discriminate between the two classes of clinically significant and nonsignificant cancer.[14] The final step is the computation of the OBM model using Bayesian optimization, which results in the best classification model and optimal hyperparameters for the model and the considered problem.

Finally, the created model was utilized to test its classification performance on an entirely independent set of patient studies set aside for testing. The sensitivity, specificity, and accuracy of prediction and the area under the receiver operating characteristic (ROC) curve were computed to describe the predictive performance of the designed model.[14] As such, using random selection, we utilized 60% of the data for training, 20% for validation, and 20% for testing. After the selection of features, the assessment of discrimination performance takes place, employing a k-fold cross-validation methodology.

Notably, no sample that contributes to training is utilized for testing, ensuring the integrity of the results. To evaluate performance, Bayesian optimization is applied to a subset of samples, whereas the remaining samples are used for assessment. This entire process is iterated across various groups. The ultimate outcomes are derived from the average of iterations where testing never involves samples used for training. Experts in machine learning with a robust statistical background meticulously designed and reviewed the procedure.

Results

Feature selection and classification

Each patient study yielded 14 intensity properties, 56 LBP texture properties, and 7560 GLCM texture properties, for a total of 7631 features per patient. Figure 2 displays exemplar slices from four different patient studies, where both the standardized mpMRI slice (top row) and the delineated PPAT region (bottom row) are shown. Figure 3 shows a heat map representing the correlation of features among each other; blue indicates a positive correlation, and red indicates a negative correlation. The heat map was clustered to show groupings of features that were similar in terms of correlation. As shown in Figure 3, large groups of features are highly correlated, suggesting that they carry redundant information.

The optimal configuration obtained using the OBM approach resulted in six features. Table 1 provides a description of the six features employed in the best classifier. Notably, all optimally selected features denote the textural properties of the PPAT region. Therefore, texture appears to have the most important discrimination capability for the two classes.

These features combined provided a classification accuracy of 0.82 with a sensitivity and specificity of 0.95 and 0.39, respectively. Table 2 gives the confusion matrix that

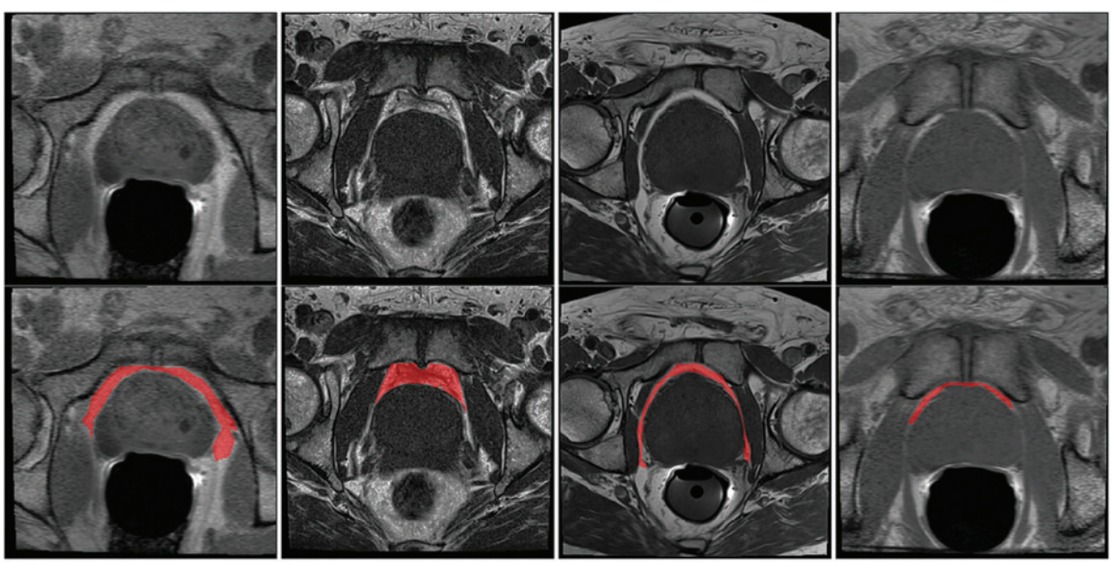

FIG. 2. Visual appearance of the PPAT region in the standardized image (*top row*) and the delineated mask (*bottom row*) for the region of interest. As can be seen, the visual appearance in different patients greatly varies.

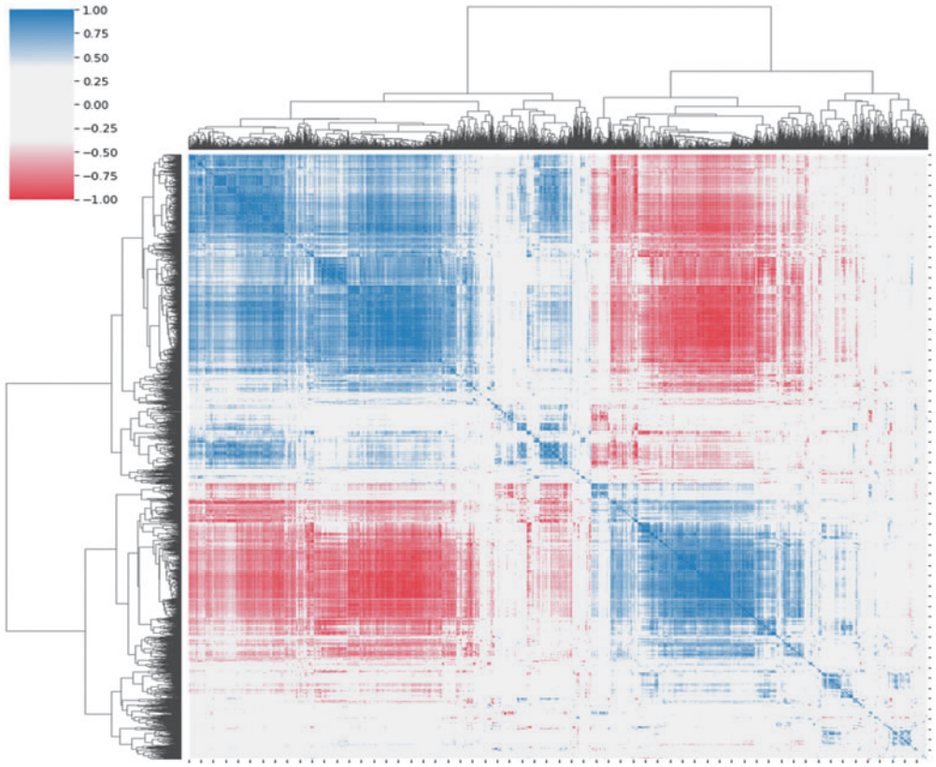

FIG. 3. Heat map representation of feature derived from PPAT regions of interest on axial T1-weighted MR images correlations expressed as a 7631 × 7631 matrix. The heat map is symmetric about the diagonal. A value of −1 means a total negative linear correlation, 0 means no correlation, and +1 means a total positive correlation.

describes the performance of the classification model built using the set of these six optimal features.

Discussion

A major challenge in PCa diagnosis is the ability to detect clinically significant cancers, avoid unnecessary biopsies, and overtreatment. In this study, we identified MRI-derived radiomic features of PPAT associated with clinically significant PCa (GS ≥7 [3 + 4]) at the final pathology analysis in a cohort of men who underwent robot-assisted prostatectomy. We referred to PPAT as surgically resectable fat during robot-assisted prostatectomy. Therefore, the PPAT was delineated volumetrically on several slice images, which differs from other studies that used only a single slice image to refer to PPAT.[6–10] We believe that accounting for fat volumetrically in 3D space instead of just one slice image allows us to account for tissue heterogeneity and increase the replicability and generalizability of our approach.

We used the OBM to identify features extracted from T1-weighted MRI scans that can classify prostate tumors into clinically significant tumors and nonclinically significant tumors. With a 98-patient training set and using features from T1-weigthed MRI sequences alone, our algorithm demonstrated discriminatory sensitivity, specificity, accuracy of prediction, and area under the ROC curve of 0.95, 0.39, 0.82, and 0.82, respectively.

The findings from our study agree with previously published literature that showed a correlation between PPAT enhancement and high GS.[17] However, in this study, the volume and thickness of PPAT were not found to be features to discriminate between clinically significant PCa of GS >7

Table 1. The Top Six Features Selected by the Optimal Biomarker Method

Rank order of feature	*Description of feature*
1	Peak intensity, GLCM with angle 180, distance 3, bins 20, window size 2 × 2, and feature 6.
2	Minimum intensity, GLCM with angle 90, distance 3, bins 10, window size 2 × 2, and feature 3.
3	Maximum intensity, GLCM with angle 90, distance 3, bins 10, window size 2 × 2, and feature 2.
4	Minimum intensity, GLCM with angle 90, distance 3, bins 10, window size 2 × 2, and feature 1.
5	Minimum intensity, GLCM with angle 45, distance 3, bins 20, window size 3 × 3, and feature 3.
6	Maximum intensity, GLCM with angle 45, distance 3, bins 20, window size 3 × 3, and feature 2.

GLCM = gray level co-occurrence matrix.

Table 2. Confusion Matrix for the Classifier Using Six Optimal Features

	Actual	
	Negative	*Positive*
Predicted		
Negative	9	4
Positive	14	71

(3 + 4), and nonclinically significant PCa. This might be attributed to the different methods used to measure PPAT volume and thickness in other studies.[6–10]

Moreover, it is noteworthy to mention that these studies used a different definition of high-grade PCa, which creates a challenge for physicians to interpret these findings, incorporate them in daily clinical practice, and replicate the findings of these studies. Therefore, in this study, we used the universal definition of clinically significant PCa of GS >7 (3 + 4).

Recent evidence has shown that PPAT modulates the prostate microenvironment by either a paracrine effect or cell-to-cell interactions.[6] Either by secreting proinflammatory and protumor adipokines, which induce inflammatory cell infiltration in the adipose tissue and destroy the extracellular matrix or through metabolic alterations, adipocytes lose their intracellular lipid content and provide exogenous fatty acids to cancer cells.[18,19]

Hence, several studies explored the qualitative changes in the peritumor adipose tissue on diagnostic imaging examination, and found correlation between several imaging parameters of the peritumor adipose tissue and disease progression, as well as expression of proinflammatory markers such as IL-6.[20–23] As such, our findings that the textural properties of the PPAT associated with clinically significant PCa might reflect qualitative changes in the PPAT that can be related to altered metabolism and presence of crown like structures.[18,19]

Our study has several limitations, including the small sample size, retrospective nature, imbalance between the groups, and use of different MRI scans. Also, our analysis did not account for different pathologic variables such as volume of tumor, percentage of GS 4, presence of lymphovascular invasion, presence of perineural invasion, or presence of a cribriform pattern. Although the proposed model used in this study is highly effective in handling many features in a complex search space, involving selection of the most relevant and potent features while ensuring stable and repeatable results with a low number of samples, it is currently limited to a binary outcome. In addition, our approach has not been externally validated. Although the performance of the method is promising, it is possible that the model was created by overfitting the training data.

This study used a novel OBM approach to identify PPAT radiomics features derived from T1-weighted MR images to distinguish patients with clinically significant PCa from those with indolent PCa. This is the first study to comprehensively examine PPAT volumetrically three dimensionally instead of relying on one image level. If our results are validated in the future on external independent data sets, we believe that the integration of our approach in daily clinical practice would help physicians avoid unnecessary biopsies and improve the decision-making process. Finally, future efforts should focus on studying the correlation of these radiomic features of PPAT with the tumor genome.

Authors' Contributions

M.S. contributed to the design implementation of the research and to the writing of the article; R.U., Y.T., and A.S. contributed to the analysis of the results and to the writing of the article; and J.K.U., D.A.T., and D.I.L. conceived the original article and supervised the project.

Data Availability Statement

Data are available upon request from the reviewer.

Ethics Approval Statement

This study was approved by the University of Pennsylvania.

Patient Consent Statement

The requirement for consent was waived.

Author Disclosure Statement

J.K.U. and D.A.T. are the cofounders of Quantitative Radiology Solutions, LLC. Other authors declare that they have no affiliations with or involvement in any organization or entity with any financial interest in the subject matter or material discussed in this article.

Funding Information

This research was partially funded by the Spanish National Program for Mobility of Professors and Researchers and the Fulbright Program, reference PRX19/00070.

Supplementary Material

Supplementary Table S1

References

1. Zhou CK, Check DP, Lortet-Tieulent J, et al. Prostate cancer incidence in 43 populations worldwide: An analysis of time trends overall and by age group. Int J Cancer 2016; 138(6):1388–1400.
2. Richenberg J, Løgager V, Panebianco V, et al. The primacy of multiparametric MRI in men with suspected prostate cancer. Eur Radiol 2019;29(12):6940–6952.
3. Jones TA, Radtke JP, Hadaschik B, et al. Optimizing safety and accuracy of prostate biopsy. Curr Opin Urol 2016; 26(5):472.
4. Retter A, Gong F, Syer T, et al. Emerging methods for prostate cancer imaging: Evaluating cancer structure and metabolic alterations more clearly. Mol Oncol 2021;15(10): 2565–2579.
5. Ahdoot M, Wilbur AR, Reese SE, et al. MRI-targeted, systematic, and combined biopsy for prostate cancer diagnosis. N Engl J Med 2020;382(10):917–928.
6. Nassar ZD, Aref AT, Miladinovic D, et al. Peri-prostatic adipose tissue: The metabolic microenvironment of prostate cancer. BJU Int 2018;121:9–21.

7. Van Roermund JG, Hinnen KA, Tolman CJ, et al. Periprostatic fat correlates with tumour aggressiveness in prostate cancer patients. BJU Int 2011;107(11):1775–1779.
8. Bhindi B, Trottier G, Elharram M, et al. Measurement of peri-prostatic fat thickness using transrectal ultrasonography (TRUS): A new risk factor for prostate cancer. BJU Int 2012;110(7):980–986.
9. van Roermund JG, Bol GH, Alfred Witjes J, et al. Periprostatic fat measured on computed tomography as a marker for prostate cancer aggressiveness. World J Urol 2010;28(6):699–704.
10. Dahran N, Szewczyk-Bieda M, Wei C, et al. Normalized periprostatic fat MRI measurements can predict prostate cancer aggressiveness in men undergoing radical prostatectomy for clinically localised disease. Sci Rep 2017;7(1): 4630; doi: 10.1038/s41598-017-04951-8
11. Nyúl LG, Udupa JK, Zhang X. New variants of a method of MRI scale standardization. IEEE Transact Med Imag 2000; 19(2):143–150.
12. Grevera, G, Udupa, J. Odhner, D, et al. CAVASS: A computer-assisted visualization and analysis software system. J Digit Imag 2007;20(Suppl 1):101–118.
13. Finley DS, Deane L, Rodriguez E, et al. Anatomic excision of anterior prostatic fat at radical prostatectomy: Implications for pathologic upstaging. Urology 2007;70(5):1000–1003.
14. Tong Y, Udupa JK, Sin S, et al. MR image analytics to characterize the upper airway structure in obese children with obstructive sleep apnea syndrome. PLoS One 2016; 11(8):e0159327.
15. Haralick RM, Shanmugam K, Dinstein IH. Textural features for image classification. IEEE Transact Syste Man Cybernet 1973;6:610–621.
16. Sonka M, Hlavac V, Boyle R. Image Processing, Analysis, and Machine Vision. Cengage Learning: Stamford, CT, USA; 2014.
17. Tafuri A, Panunzio A, Greco F, et al. MRI-derived apparent diffusion coefficient of peri-prostatic adipose tissue is a potential determinant of prostate cancer aggressiveness in preoperative setting: A preliminary report. Int J Environ Res Public Health 2022;19(23):15996.
18. van Roermund JG, Hinnen KA, Tolman CJ, et al. Periprostatic fat correlates with tumour aggressiveness in prostate cancer patients. BJU Int 2011;107(11):1775–1779.
19. Feng S, Lou K, Luo C, et al. Obesity-related cross-talk between prostate cancer and peripheral fat: Potential role of exosomes. Cancers 2022;14(20):5077.
20. Gregg JR, Surasi DS, Childs A, et al. The association of periprostatic fat and grade group progression in men with localized prostate cancer on active surveillance. J Urol 2021;205(1):122–128.
21. Nieman KM, Romero IL, Van Houten B, et al. Adipose tissue and adipocytes support tumorigenesis and metastasis. Biochim Biophys Acta 2013;1831(10):1533–1541.
22. Zhai T, Hu L, Ma W, et al. Peri-prostatic adipose tissue measurements using MRI predict prostate cancer aggressiveness in men undergoing radical prostatectomy. J Endocrinol Invest 2021;44(2):287–296; doi: 10.1007/s40618-020-01294-6
23. Ahn H, Lee JW, Jang SH, et al. Prognostic significance of imaging features of peritumoral adipose tissue in FDG PET/CT of patients with colorectal cancer. Eur J Radiol 2021;145:110047.

Address correspondence to:
Jayaram K. Udupa, PhD, LFIEEE, FAIMBE
Medical Image Processing Group
Department of Radiology
University of Pennsylvania
3710 Hamilton Walk
Goddard Building, 6th Floor, Room 601W
Philadelphia, PA 19104
USA

E-mail: jay@pennmedicine.upenn.edu

Drew A. Torigian, MD, MA, FSAR
Medical Image Processing Group
Department of Radiology
University of Pennsylvania
3710 Hamilton Walk
Goddard Building, 6th Floor, Room 601W
Philadelphia, PA 19104
USA

E-mail: drew.torigian@pennmedicine.upenn.edu

Abbreviations Used

CAVASS = Computer-Aided Visualization and Analysis Software System
GLCM = gray level co-occurrence matrix
LBP = local binary pattern
MIPG = Medical Image Processing Group
mpMRI = multiparametric magnetic resonance imaging
MRI = magnetic resonance imaging
OBM = optimal biomarker
PCa = prostate cancer
PPAT = periprostatic adipose tissue
ROC = receiver operating characteristic
ROI = region of interest